

# Effect of Combustion on Mixing by Opposed Jets

Takahisa Nagao and Shinsuke Matsuno  
IHI Corporation

1, Shin-nakahara-Cho, Isogo-ku, Yokohama, Kanagawa 235-8501, Japan

A. Koichi Hayashi

Aoyama Gakuin University

5-10-1 Fuchinobe, Chuo, Sagami-hara, Kanagawa 252-5258, Japan

## 1 Introduction

Every year, operating temperatures of combustors are being raised to enhance the efficiency of gas turbine engines. Hence, reducing the size and mass of a combustor is desirable to make the combustor. However, reducing the combustor size negatively influences the temperature distribution at the exit of the combustor. Turbine blades can be damaged if the exhaust gas creates “hot spots,” which are areas of extremely high temperature. Thus, the temperature distribution at the combustor exit should be equalized during gas turbine engine development.

Figure 1 shows a common rich-burn quick-quench lean-burn (RQL) combustor<sup>3</sup>. Aircraft engines generally have an annular shape. In the fuel-rich primary zone, the injected fuel is burned with swirling air. Downstream of the primary zone, additional air is required to complete the combustion process. In this type of combustor, the temperature distribution of the combustor is controlled with additional air. Therefore, discussing the details of the flow field is important.

Figure 2 shows a typical image of jet mixing in a cross flow. According to Holdeman et al.<sup>4,5</sup>, jet penetration and mixing are characterized by the hole shape, hole diameter, hole spacing, duct height, and momentum flux ratio. This group studied a time-averaged concentration. Very little research on the behavior of unsteady jet mixing exists.

Hussain<sup>6</sup>, Andreopoulos<sup>7</sup>, and Fric and Roshiko<sup>8</sup> discussed the detailed mixing behavior of jet and cross flows. Investigating the mixing in a combustor is important. Mare et al.<sup>9</sup> simulated a can-type combustor and discussed the mixing characteristics. In fact, real combustors consist of swirled air, dilution air, film cooling air and elsewhere. These components should be evaluated independently.

In our previous study<sup>10</sup>, we examined the mixing of opposed jets in a rectangular duct, which is a simplified shape of a gas turbine combustor. An experiment and simulation were performed. The large eddy simulation (LES) result qualitatively agreed with the experiment. A simulation was carried out to examine the effect of momentum flux ratio  $J$ :

$$J = \frac{\rho_j u_j^2}{\rho_m u_m^2}, \quad (1)$$

where  $\rho$  is the density,  $u$  is the velocity, subscript  $j$  denotes the jet, and subscript  $m$  denotes the main stream.

Figure 3 shows the effect of the momentum flux ratio on unmixedness ( $U_s$ ); the case of  $J = 4$  has especially high  $U_s$ . Figure 4 shows that the mixing behavior can be classified into three types

depending on the duct shape and flow conditions. At  $J = 4$ , the two jets do not collide because the jet penetration is weak, and thus, the mixing is not improved. On the other hand, the jet is dispersed and deflected by the opposing jet when  $J = 9$ . When  $J = 16$  and  $64$ , a radial jet is generated at the collision plane. The radial jet fluctuates due to the instability of the opposed jets. The high mixing rate is due to the radial jet instability. However, these results are obtained using non-reaction flows.

This study examined the effectiveness of reactions: non-reactive cases were compared to reactive cases. The momentum flux ratio  $J$  was selected for the jet collisions based on the previous study.

## 2 Numerical Model and Method

Figure 4 depicts the target geometry. As discussed in the previous section, the flow field consists of a rectangular duct and opposed jets. The left side of the duct is the inlet of the main stream, and the right side is open to the atmosphere. Figure 5 shows the numerical model. The origin point is the center of the duct on the centerline of the jet inlet. The minimum numerical mesh length is 0.1 mm, and the maximum length is 1 mm. There are 3 million grid points.

The numerical methods are given in Table 1. The commercial CFD code Advance Soft Front Flow Red 4.1 was used for the LES computation. The code was developed for a Japanese government project. Presently, some companies and universities are continuing development on it.

The Navier-Stokes equation and LES dynamic SGS model are used. In the LES, the spatially filtered continuity, Navier-Stokes equations, and flamelet scalar equation are respectively given as

$$\frac{\partial \bar{u}_i}{\partial t} + \frac{\partial \bar{u}_i \bar{u}_j}{\partial x_j} = -\frac{1}{\rho} \frac{\partial \bar{p} \delta_{ij}}{\partial x_j} + \nu \frac{\partial}{\partial x_j} \left[ \frac{\partial \bar{u}_i}{\partial x_j} + \frac{\partial \bar{u}_j}{\partial x_i} \right] - \frac{\partial}{\partial x_j} (\bar{u}_i \bar{u}_j - \bar{u}_i \bar{u}_j) \quad (2)$$

$$\frac{\partial}{\partial t} \bar{\rho} \bar{\xi} + \frac{\partial}{\partial x_j} \bar{\rho} \bar{u}_j \bar{\xi} = \frac{\partial}{\partial x_j} \left( \frac{\mu_{SGS}}{\rho_{SGS}} \frac{\partial \bar{\xi}}{\partial x_j} \right) \quad (3)$$

$$\tau_{ij} = (\bar{u}_i \bar{u}_j - \bar{u}_i \bar{u}_j) - \frac{2}{3} \delta_{ij} q. \quad (4)$$

The subgrid-scale (SGS) eddy viscosity is modeled by the standard Smagorinsky model as

$$\tau_{ij} = 2C\bar{\Delta}^2 |\bar{S}| \bar{S}_{ij}. \quad (5)$$

where  $C$  is the Smagorinsky coefficient and  $\Delta$  is the length scale of the SGS turbulence.

In this study,  $C$  was calculated with the dynamic SGS model<sup>10</sup>, which was developed by Germano and Lilly. The laminar flamelet model was used as the combustion model ( $\xi_i = 0$ : jets,  $\xi_i = 1$ : main stream). Figure 6 shows the flamelet functions that were calculated using GRI-Mech 3.0 under the conditions given in Table 2. Mare et al.<sup>9</sup> reported that the flamelet assumption qualitatively agrees with the experiment results excluding the high strain rate region, especially around the swirler.

The simulation was validated for non-reaction flow in our previous study<sup>11</sup>. However, the experiments on combustion were not completed. Further studies are needed to validate the simulation for combustion flows.

## 3 Results and Discussion

Table 2 presents the calculated conditions. Figure 7 shows the effect of the momentum flux ratio on unmixedness. The distributions of the time-averaged and fluctuation RMS results over the cross-section of the jet inlet centerline are shown in Figures 8–11.

For a detailed discussion, unmixedness is defined as follows:

$$U_s = \frac{C_{rms}}{C_{avg}} \quad (6)$$

$$C_{rms} = \sqrt{\frac{1}{n} \sum_{i=1}^n (C_i - C_{avg})^2} \quad (7)$$

where  $U_s$  is the spatial unmixedness parameter<sup>1,2</sup>,  $C_{avg}$  is the averaged temperature upon exit,  $C_{rms}$  is the root mean square of temperature,  $n$  is the number of numerical cells in each cross section, and  $C_i$  is

the temperature in a numerical cell

Unmixedness is examined in terms of the time-averaged results. In Figure 7, unmixedness is normalized by  $U_{s0}$ , which is the unmixedness for the cross section of  $x = 0$  (location of jet inlets). The unmixedness in the reactive case is larger than in the non-reactive case for the same cross section, as shown in Figure 7(a). However, combustion increases the fluid volume and velocity. Hence, considering mixing phenomena for which the residential time is on the horizontal axis is reasonable. Figure 7(b) shows a small gap between the reactive and non-reactive cases.

Figures 8–10 show differences between the reactive and non-reactive cases. These differences are due to the reaction heat, which increases the fluid temperature and volume. The temperature and velocity increased with the flow downstream in the reactive case. This result suggests that the reaction inside the duct remains incomplete. The temperature fluctuation RMS is larger than that in the non-reactive case, downstream of the opposed jets. The high RMS of the temperature region indicates a high reaction rate or high mixing rate. Since a high mixing rate is caused by high velocity fluctuation, as shown in Figure 11, the high temperature RMS is likely to be due to the high reaction rate downstream of the opposed jets.

Note that the velocity fluctuation RMSs are qualitatively the same in Figures 11(a) and (b). This demonstrates that fluid mixing does not differ in the reactive and non-reactive cases. Therefore, the results suggest that the reaction does not have a large effect on fluid mixing.

Figure 12 shows the instantaneous temperature distribution. The outer periphery of the opposed jets in the reactive case is more stable than in the non-reactive case. This is associated with molecular viscosity; however, there seems to be no effect of molecular viscosity on mixing.

This study was performed under only one condition. Thus, further studies are needed to estimate the effects of the reaction.

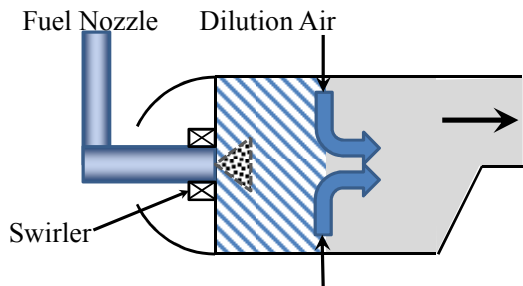


Figure 1. Jet engine combustor

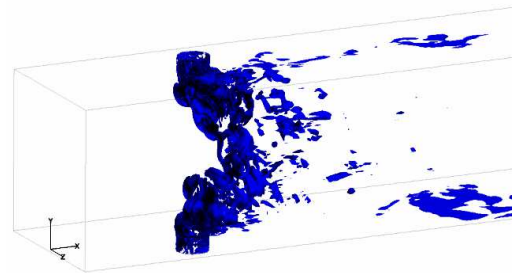
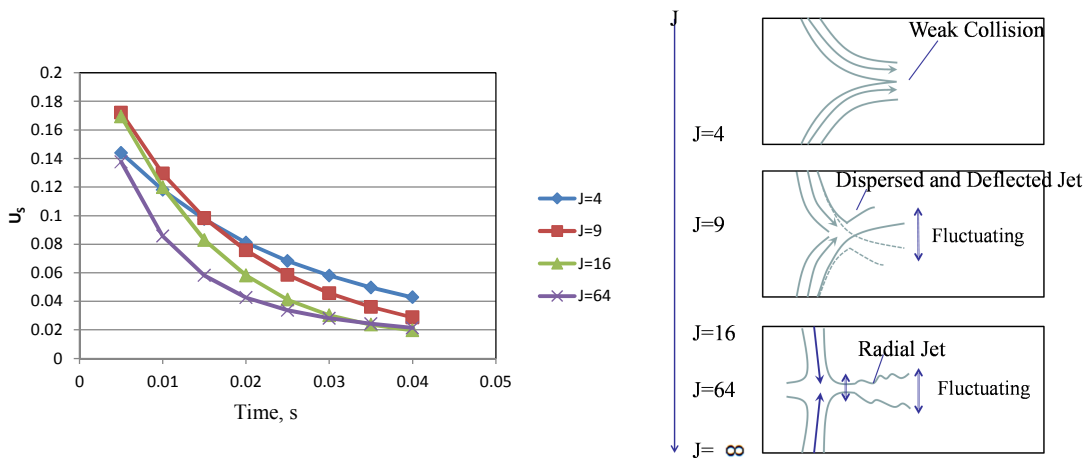


Figure 2. Jet mixing with opposite impinging jets



(a) Effect of momentum flux ratio on unmixedness

(b) Suggested mechanism of opposed jet mixing

Figure 3. Previous work in our laboratory<sup>11</sup> ( $D/H = 0.2$ ,  $W/H = 1$ , non-reactive)

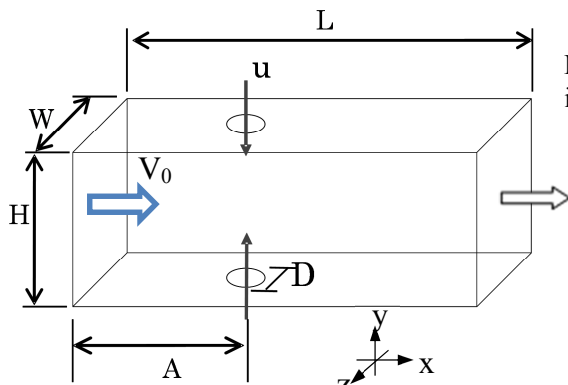


Figure 4. Outline of flow passage (A = 100, D = 14, L = 300, W = 50, H = 50)

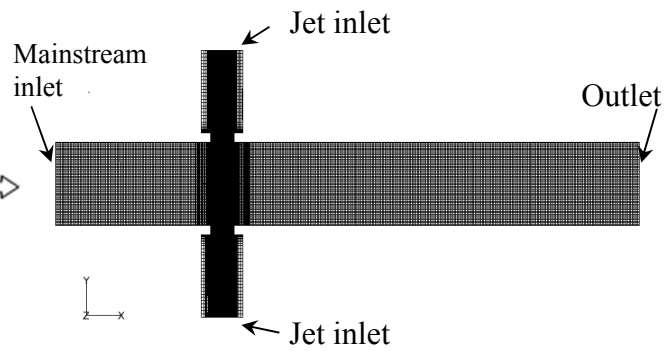
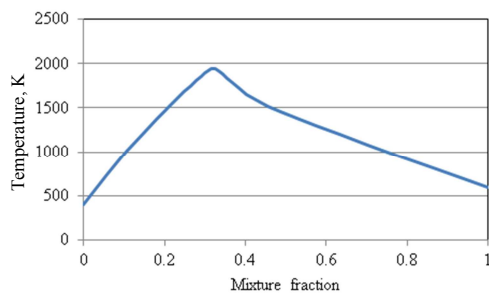
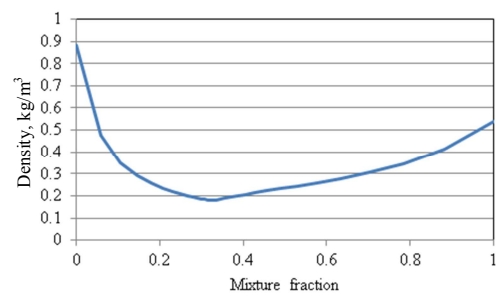


Figure 5. Numerical geometry model (cross section of jet inlets centerline, xy plane)

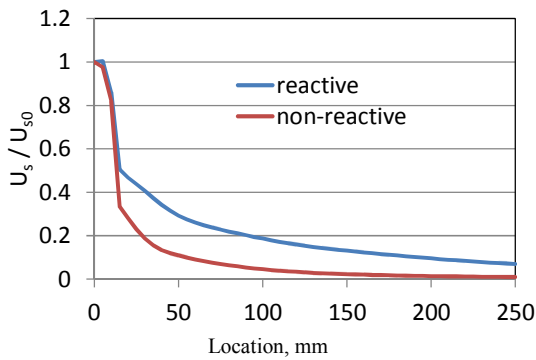


(a) Temperature

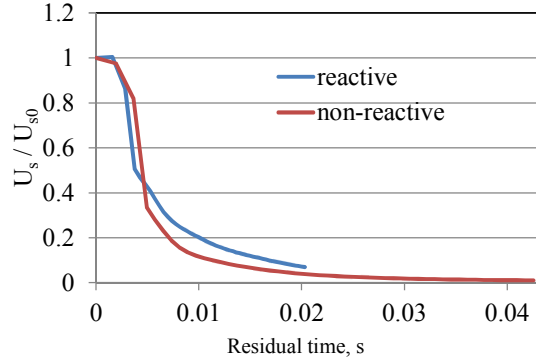


(b) Density

Figure 6. Laminar flamelet functions



(a) Horizontal axis: location



(b) Horizontal axis: residual time

Figure 7. Effect of reaction on unmixedness

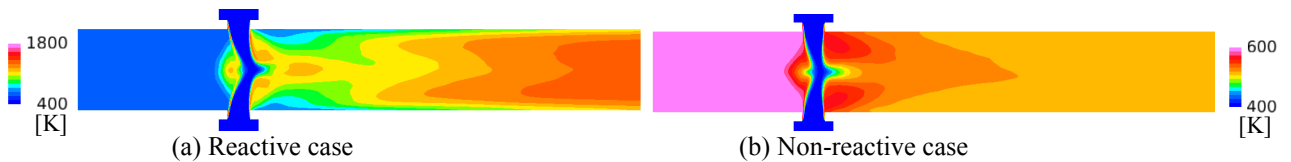


Figure 8. Temperature distribution (xy plane)

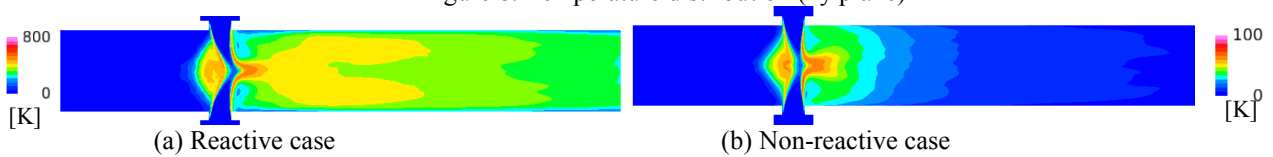


Figure 9. RMS of temperature distribution fluctuation (xy plane)

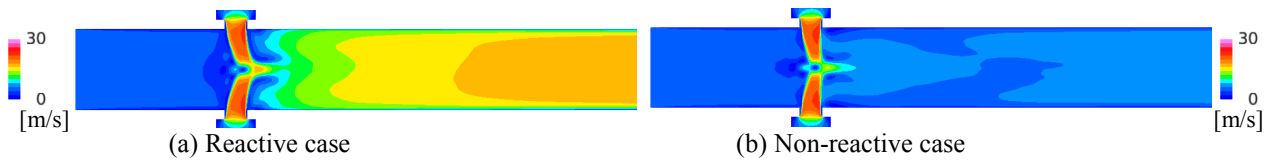


Figure 10. Velocity magnitude distribution (xy plane)



Figure 11. RMS of velocity magnitude distribution fluctuation (xy plane)

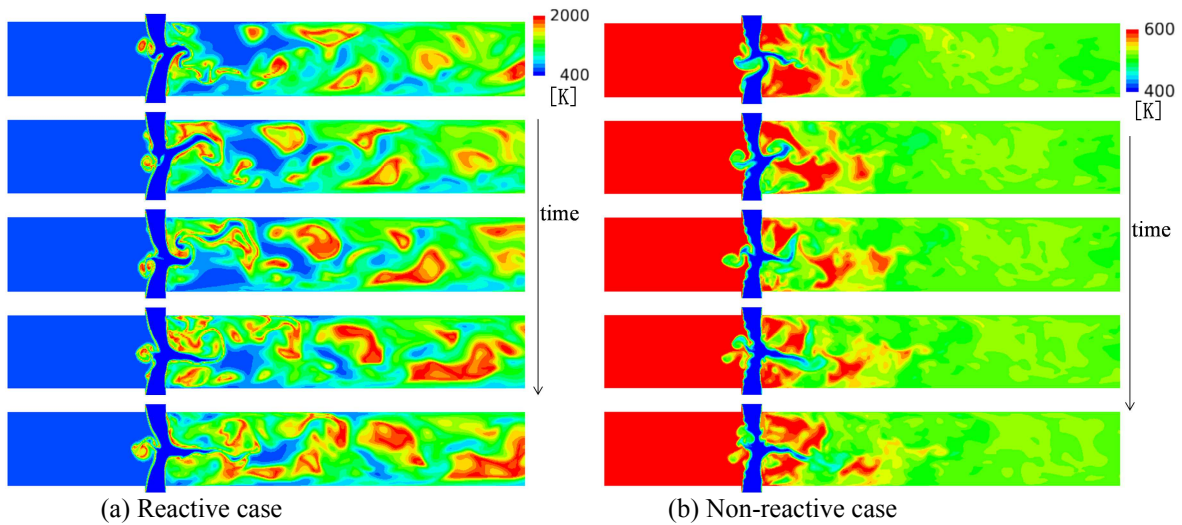


Figure 12. Instantaneous temperature distribution (time interval = 160 micro second)

Table 1. Numerical methods and mesh condition

CFD Code	AdvanceSoft Advance/FrontFlow/Red 4.1	Wall	Spalding law, thickness of first layer = 0.1 mm
Equation	Incompressible Navier–Stokes	Cell	Unstructured
Fluid	Incompressible perfect gas	Discretization	Blended second-order central with first-order upwind (8: 2)
Turbulent	LES dynamic SGS	Parallelization	Region splitting (METIS), MPI-Infiniband, 96 CPUs
Combustion	Laminar flamelet	Number of cells	3 million
Jet inlet	Random perturbations <sup>12</sup>	Min. $\Delta x$	0.1 mm
Mainstream inlet	Uniformity velocity	Ave. $\Delta x$	1 mm

Table 2. Calculated conditions

Momentum flux ratio $J$	8.93	Equivalence ratio $\phi$	4.0
Jet velocity $V_j$ [m/s]	10	Mainstream Velocity $V_m$ [m/s]	4.331
Jet temperature $T_j$ [K]	400	Mainstream Temperature $T_m$ [K]	600
Jet component [weight%]	O <sub>2</sub> (23.3%) N <sub>2</sub> (76.7%)	Mainstream Component [Weight%]	CH <sub>4</sub> (12.4%) N <sub>2</sub> (87.6%)

## References

- [1] Hatch, M.S., Sowa, W.A., Samuelsen, G.S., Holdeman, J.D., "Jet mixing into a heated cross flow in a cylindrical duct: influence of geometry and flow variations," AIAA Paper 92-0773, Reno, Nevada, Jan. 6–9, 1992 (also NASA TM 105390).
- [2] Lincinsky, D.S., True, B., Vranos, A., and Holdeman, J.D., "Experimental study of cross-stream mixing in a rectangular duct," NASA Technical Memorandum 105694, AIAA-92-3090.
- [3] Lefebvre, A.H., and Ballal, D.R., CRC Press, "Gas Turbine Combustion," third edition, 2010.
- [4] Holdeman, J. D., and Walker, R. R., and Kors, D. L., "Mixing of multiple dilution jets with a hot primary airstream for gas turbine combustors," AIAA Paper 73-1249, 1973.
- [5] Holdeman, J. D., and Walker, R. R., and Kors, D. L., "Mixing of a row of jets with a confined crossflow," AIAA Journal, vol. 15, no. 2, pp. 243–9, 1977.
- [6] Hussain, A.K.M.F., "Coherent structures and turbulence," Journal of Fluid Mechanics, vol. 173, pp. 303-356, 1986.
- [7] Andreopoulos, J., "On the structure of jets in a crossflow," Journal of Fluid Mechanics, vol. 157, pp. 163-197, 1985.
- [8] Fric, T.F. and Roshiko, A., "Vortical structure in the wake of a transverse jet," Journal of Fluid Mechanics, vol. 279, pp. 1-47, 1994.
- [9] Mare, F. di, Jones, W. P. and Menzies, K. R., "Large eddy simulation of a model gas turbine combustor," Combustion and Flame, vol. 137, pp. 278-294, 2004.
- [10] Lilly, D.K., "A proposed modification of the Germano subgrid-scale closure model," Physics of Fluids, vol. 4, pp. 633-635, 1992.
- [11] Nagao, T., "Fluid mixing of opposed jet flows in the rectangular duct," Proceedings of AIAA Aerospace Science Meeting, January 2013.